Photochemical & Photobiological Sciences

PAPER

View Article Online
View Journal | View Issue

Cite this: *Photochem. Photobiol. Sci.*, 2014, **13**, 603

Photoswitchable fluorescent diheteroarylethenes: substituent effects on photochromic and solvatochromic properties†

Florencia Gillanders,[a,b] Luciana Giordano,‡[a] Sebastián A. Díaz,[a] Thomas M. Jovin*[a] and Elizabeth A. Jares-Erijman§[b]

Received 25th October 2013,
Accepted 5th January 2014

DOI: 10.1039/c3pp50374g

www.rsc.org/pps

Photoswitchable fluorescent diheteroarylethenes are promising candidates for applications in super-resolution molecular localization fluorescence microscopy thanks to their high quantum yields and fatigue-resistant photoswitching characteristics. We have studied the effect of varying substituents on the photophysical properties of six sulfone derivatives of diheteroarylethenes, which display fluorescence in one (closed form) of two thermally stable photochromic states. Electron-donating substituents displace the absorption and emission spectra towards the red without substantially affecting the fluorescence quantum yields. Furthermore, ethoxybromo, a very electron-donating substituent, stabilizes the excited state of the closed isomer to the extent of almost entirely inhibiting its cycloreversion. Multi-parameter Hammett correlations indicate a relationship between the emission maxima and electron-donating character, providing a useful tool in the design of future photochromic molecules. Most of the synthesized compounds exhibit small bathochromic shifts and shorter fluorescence lifetimes with an increase in solvent polarity. However, the ethoxybromo-substituted fluorescent photochrome is unique in its strong solvatochromic behaviour, constituting a photoactivatable (photochromic), fluorescent and highly solvatochromic small organic compound. The Catalán formalism identified solvent dipolarity as the principal basis of the solvatochromism, reflecting the highly polarized nature of this molecule.

Introduction

The dramatic improvements in the spatial resolution achieved in fluorescence microscopy beyond the limits imposed by optical diffraction[1,2] have been based on two approaches. The first employs a deterministic spatio-temporal engineering of photophysical dynamics, as in stimulated emission depletion (STED[3]) and structured illumination (SIM[4,5]). In the alternative strategy of single molecule localization microscopy (SMLM[6]), one evaluates the spatial distribution of detected photons originating stochastically from individual fluorophores so as to establish their 2D or 3D positions accurately and precisely (<50 nm uncertainty). Other super-resolution techniques assess fluctuation statistics or introduce nonlinear features in wide-field microscopy, but do not localize single molecules and achieve moderate albeit useful degrees of 2D or 3D resolution enhancement (SOFI;[7] ISM[8,9]).

The two major implementations of SMLM – fluorescence photoactivation localization (PALM[10]), stochastic optical reconstruction (STORM[11]) and their variants[12] – utilize probes undergoing irreversible or reversible transitions between dark and emissive excited states and their corresponding ground states.[13,14] In addition to the generic requirement of brightness (large absorption cross-section and quantum yield), high contrast (on/off ratio), and photostability, probes must exhibit thermal stability of both dark and emitting states and, in many applications, a high resistance to fatigue during photoswitching, *i.e.* the ability to undergo numerous reversible cycles of photoconversion. The class of fluorophores that exhibit light-dependent interconversions of this nature include fluorescent proteins,[15,16] nanoparticles,[17,18] and organic dyes.[19,20] The latter are most often subjected to fine control by exposure to reagents affecting redox states[12,21] and excited state dynamics.[19,22] Such chemical modifications are spatially and temporally stochastic in nature, hindering the integration of the SIM and SMLM techniques, a major objective of our

[a]*Laboratory of Cellular Dynamics, Max Planck Institute for Biophysical Chemistry, Am Fassberg 11, 37077 Göttingen, Germany. E-mail: tjovin@gwdg.de*
[b]*Departamento de Química Orgánica, Facultad de Ciencias Exactas y Naturales, Universidad de Buenos Aires, CIHIDECAR, CONICET, 1428 Buenos Aires, Argentina*
† Electronic supplementary information (ESI) available: Synthetic procedures; ^{1}H and ^{13}C NMR spectra for compounds; description of Hammett constant calculation; linear fits equation for Fig. 2; solvent dependence tables; Catalán fits; photoconversion calculations; fatigue and photocycles; custom built spectrometer and photoconversion apparatus overview. See DOI: 10.1039/c3pp50374g
‡ Present address: Centro de Investigaciones en Bionanociencias (CIBON), CONICET, Godoy Cruz 2390, 1425 Capital Federal, Argentina.
§ Deceased September 29, 2011.

laboratory in connection with live cell optical sectioning microscopy based on programmable structured illumination.[23]

Diarylethene derivatives possess very efficient, reproducible and fatigue resistant photochromicity – a bimodal, reversible, photo-induced transition between two states with different absorption properties. When paired with a fluorescent donor, diarylethenes can act as switchable Förster resonance energy transfer (FRET) acceptors. Varied constructs including organic dyes[24] or quantum dots[25] as donors have been reported in the literature. We have denoted this phenomenon as photochromic FRET[24] (pcFRET), and it has been successfully utilized for selective modulation in phase-sensitive microscopy.[26]

High-speed interrogation and functional control of molecules at deterministic positions in space and time are best achieved with small, chemically simple probes that undergo efficient photoconversion. Photochromic FRET probes are by definition composed of at least dyads, generally resulting in a fairly large molecular structure. In the work reported here, we have attempted to maintain the pcFRET functionality by exploiting a new type of diheteroarylethene derivative that incorporates both the properties of fluorescence and photochromicity. The sulfone derivative of the photochromic diheteroarylethene 1,2-bis(2-methyl-1-benzothiophen-3-yl)perfluorocyclopentene[29] exhibits the characteristic changes in absorption spectra upon cyclization and cycloreversion typical of diheteroarylethenes but is also fluorescent in the closed form. The latter is generated by irradiation of the open isomer with UV light. Irradiation with visible light (>400 nm) restores the molecule to its open form.

In an attempt to maximize the high quantum yields and fatigue-resistant photoswitching characteristics of the fluorescent photochromes, we studied the effect of aryl substituents at positions 6 and 6′ of the benzothiophene rings of 1,2-bis(2-methyl-1-benzothiophen-1,1-dioxide-3-yl)perfluorocyclopentene (**1**) on the spectroscopic and photochemical properties of the molecule. Similar studies have been carried out on non-fluorescent diheteroarylethenes with different heterocyclic side groups[30,31] and with varying substitutions at the reactive carbon[32] and at positions on the conjugated aryl ring.[33] Irie *et al.*[34] found that electron-donating substituents positioned on the aryl ring *para* to the thiophenes of non-fluorescent diheteroarylethenes increased the absorption coefficients and decreased the cycloreversion quantum yields. Uno *et al.*[27] reported that phenyl and thiophene groups increase fluorescence quantum yields, but that the latter decrease in polar solvents. Takagi *et al.* have recently reported[35] the effect of alkyl group substitutions at the reactive carbon on the fluorescence of a derivative of **1**. Alkyl chains with two or more carbon atoms were found to protect the sulfone groups from the attack of polar solvent molecules, thereby reducing the efficiency of the non-radiative deactivation pathways associated with the sulfone group and increasing quantum yields. In this study, we evaluated the effects of six substituents with a range of electron donating/withdrawing functional groups in position *para* to the coupling site of the aryl rings at positions 6 and 6′ of **1** on the spectroscopic and photoconversion properties, including solvatochromicity.

Results and discussion

Six derivatives of **1** were synthesized according to Scheme 1. *para*-Substituted arylboronic acids with substituents ranging from moderately electron-withdrawing (cyano) to electron-donating (ethoxybromo) were chosen and coupled to **2**, the iodated derivative of **1**, *via* the Suzuki reaction to give compounds **3–8**. No relationship was evident between the required reaction conditions and the electron-withdrawing character of the boronic acid substituents. The conversion of the open forms which only absorb at <400 nm to the closed forms upon irradiation with UV light (Scheme 2) was manifested by a

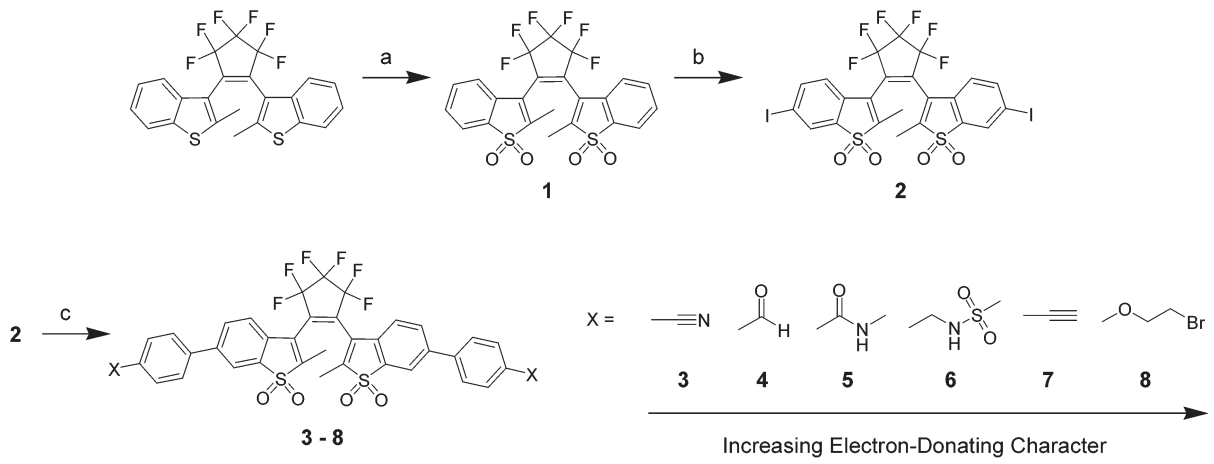

Scheme 1 Synthesis of compounds **3–8**. Reaction conditions: (a) H_2O_2, AcOH (glacial), reflux, 80%; (b) I_2, H_5IO_6, H_2SO_4, 92%; (c) $B(OH)_2$-Ar-X, $Pd_2(bda)_3$, $P(C_6H_{11})_3$, THF, K_2CO_3 (ss), 40–70% (for **5**, **6** and **8**, protocol adapted from Uno *et al.*[27]) or $B(OH)_2$-Ar-X, $Pd(AcO)_2$, K_2CO_3, THF–ethanol–H_2O, 60–90% (for **3**, **4** and **7**, protocol adapted from Qiu *et al.*[28]). Substituents ordered from **3** to **8** in approximately increasing electron donating character.

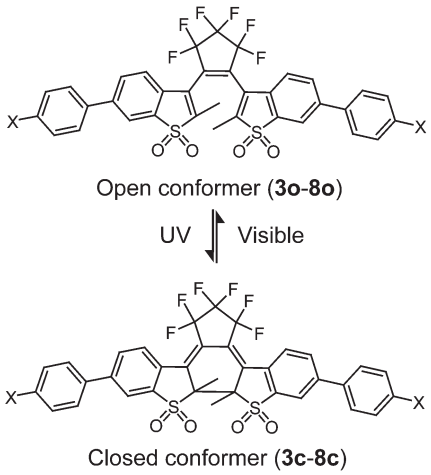

Scheme 2 Structures of the open (**3o–8o**) and closed (**3c–8c**) isomers. Cyclization (**o** → **c**) was carried out by irradiation with UV light (<400 nm) and cycloreversion (**c** → **o**) with visible light (~450 nm).

reduced absorption at the open isomer maximum and a new absorption band near 450 nm.

In order to evaluate the spectroscopic data and the photoconversion characteristics of **3–8**, three models were used: Hammett correlations,[36] an approximation of the potential energy surface diagram of diheteroarylethenes; and the Catalán formalism. The following brief introductions to each model are intended to facilitate the interpretation of the results.

Hammett correlations were utilized to evaluate the relationship between the photophysical properties of the probes and the electronic nature of the substituents. The Hammett equation[37] relates the equilibrium constant to the kinetic constant of the ionization reaction of *para* and *meta* substituted benzoic acids, allowing conclusions to be reached regarding the influence of the substituent on the acidity of the molecules. The difference between the equilibrium constants of substituted and non-substituted benzoic acid is proportional to the kinetic constant of ionization multiplied by an arbitrary constant (σ), which can be assumed to depend solely on the identity of the substituent, and therefore used to study different systems. Hammett[37] and Hansch *et al.*[36] have compiled extensive lists of σ values for many functional groups. Other measurements, for example ^{19}F (for fluor-substituted compounds) or ^{13}C NMR shifts, can complement or substitute the Hammett analysis.[38,39] In our case, shifts in NMR spectra were more easily obtained from ^{13}C than from ^{19}F NMR for the substituents of **3–8**.[40,41] The shift of the carbon in position *para* to the substitution (C3 in Scheme S1†) was divided by the shift of a carbon atom in benzene and this was used as the Hammett parameter σ'. A value of $\sigma' > 1$ implies a shift towards stronger magnetic fields for C3 and consequently less electron density on that carbon, indicative of an electron-withdrawing character of the substituent. Values of $\sigma' < 1$ denote carbon shifts towards lower field strength and, therefore, an electron-donating character.

We invoked *ab initio* MO studies[42,43] and molecular dynamics calculations[44] of *cis*-1,2-(3,3′-dithienyl)ethylene as a model for the diarylethene family, and a qualitative representation of the potential energy surfaces (PES) is given in Scheme 3. The ground state PES presents two local minima corresponding to the open and closed isomers. The excited state PES features a local minimum with a geometry similar to that of the ground state closed isomer, and another local minimum with an inter-reactive-carbon bond length similar to that of the ground state transition state, but with a geometry similar to that of the ground state open isomer.[42] A conical intersection (CI) in close proximity to the latter minimum is proposed as the main pathway for both cyclization and cycloreversion reactions.[44,45]

Due to their extended hydrocarbon structure diheteroarylethenes are known to be fairly insoluble in water and exhibit low fluorescence quantum yields and very poor photoconversion characteristics.[46] Solvents were thus selected over a wide range of polarities so as to investigate to what degree solvent polarity affected the key photophysical properties. The E_T^N (normalized molar electronic transition) scale of solvent polarity[47] was used to compare the given properties in microenvironments varying polarity of the environment. To elucidate the nature of the solvent effects, the Catalán formalism was used.[48] This relation divides the global solvent effects into four parameters: two general effects – solvent polarizability (SP) and dipolarity (SdP) – and two specific interactions – solvent acidity (SA) and basicity (SB). A linear regression is performed according to eqn (1), in which y is the spectroscopic observable of interest, SP, SdP, SA, and SB solvent-tabulated reference values, and a–d the corresponding weighing coefficients.

$$y = y_0 + a_{SP}SP + b_{SdP}SdP + c_{SA}SA + d_{SB}SB \quad (1)$$

Details of the procedures and fits are described in section 7 of the ESI.† To summarize, regressions with all four parameters

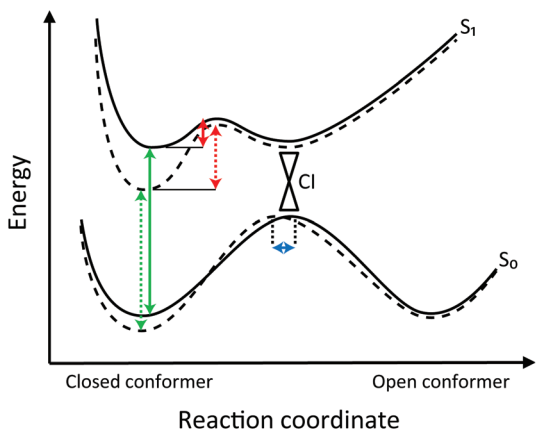

Scheme 3 Changes in qualitative potential energy surface of modified diheteroarylethenes. Potential energy surfaces without (solid line) and with (dashed line) the presence of electron-donating substituents indicating the proposed emission wavelength increase (green), the excited state transition energy increase (red) and the ground state transition coordinates shift (blue). Adapted from Takagi *et al.*[35]

were calculated; those with a p-value >0.25 were excluded and the fit was repeated, thereby retaining only the parameters making a significant contribution.[49]

Spectroscopic properties

The absorption spectra of both open (**o**) and closed (**c**) forms of **3–8** and the emission spectra of the closed isomers in ethyl acetate are shown in Fig. 1. The degree of photoconversion for all compounds was close to unity, reflecting a very efficient generation of the closed isomer from the open isomer upon irradiation. In other words, the photostationary state induced by UV light is highly biased towards cyclization, implying that UV-induced cycloreversion is close to negligible for this family of compounds.[27,50] The spectroscopic properties of all compounds in ethyl acetate are listed in Table 1. A clear bathochromic shift of the absorbance maxima was observed, with peak wavelengths increasing with a greater electron-donating character of the substituent. For example, the absorbance maximum of the second absorption band of the open form in ethyl acetate increased steadily from 327 nm for **3o** to 351 nm for **8o**. Similarly, a shift of 36 nm was observed between the absorbance maxima of **3c** and **8c**. A very large bathochromic shift in the fluorescence maximum from 510 to 589 nm was also observed between **3c** and **8c**. Fluorescence quantum yields were 2 to 5 times greater than that of compound **1** (no substituent, Φ_f = 0.12 in ethyl acetate[27]). However, there was no correlation between the values and electron-donating character, although the fluorescence lifetimes were clearly affected by the substituent character, increasing more than two-fold from 1 ns for **3c** to 2.2 ns for **8c**.

Table 1 Spectroscopic properties of **3–8** in ethyl acetate and corresponding ^{13}C NMR Hammett constants

		Open-ring isomer (**o**)	Closed-ring isomer (**c**)			
	σ'	λ_{max} (nm), ε (mM^{-1} cm^{-1})	λ_{max} (nm), ε (mM^{-1} cm^{-1})	λ^{em}_{max} (nm)	Φ_f	τ_f (ns)
3	1.04	294, 17; 327, 12	436, 36	510	0.29	1.1
4	1.05	297, 32; 331, 22	441, 43	516	0.34	1.2
5	1.02	299, 17; 330, 12	441, 36	521	0.20	1.3
6	1.00	289, 18; 333, 15	446, 38	532	0.31	1.2
7	1.00	300, 17; 334, 12	451, 44	535	0.31	1.6
8	0.95	308, 14; 351, 12	472, 40	589	0.57	2.2

σ' = ^{13}C NMR Hammett constant; λ_{max} = absorption maximum; ε = molar absorption coefficient; λ^{em}_{max} = fluorescence emission maximum; Φ_f = fluorescence quantum yield; τ_f = fluorescence lifetime.

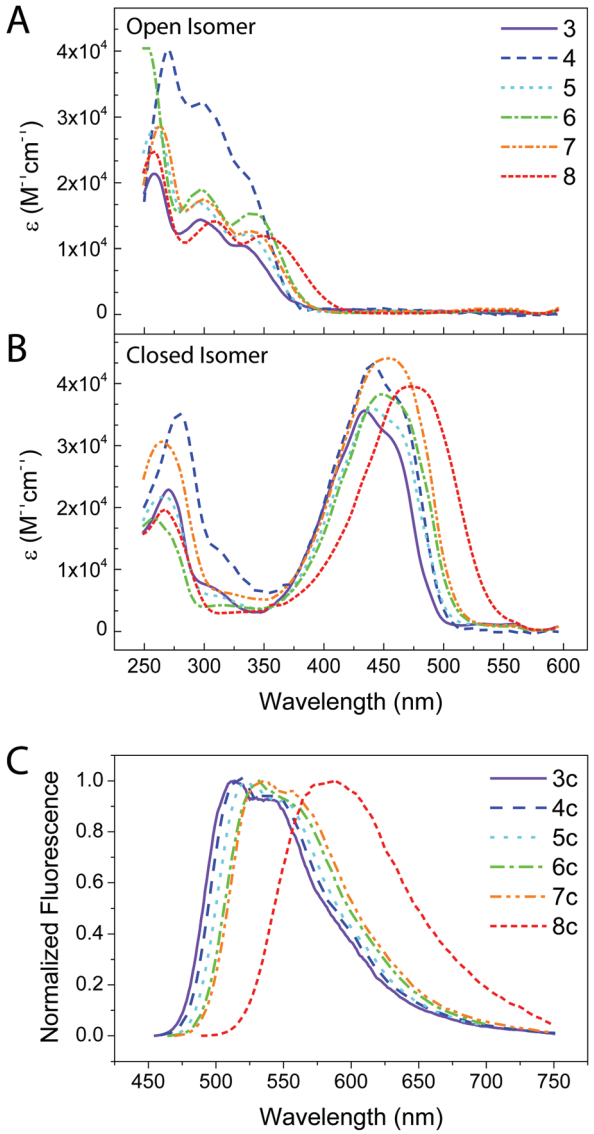

Fig. 1 Molar extinction coefficients (ε, M^{-1} cm^{-1}) for (A) open and (B) closed isomers of **3–8** in ethyl acetate. (C) Normalized fluorescence emission spectra of **3c–8c** in ethyl acetate excited at their respective absorption maxima.

To quantitate the weights of the substituent effects, the absorbance and emission maxima of **3c–8c** in 1,4-dioxane were plotted against the Hammett parameter σ' (Fig. 2). Given the extended conjugation of π orbitals present in the closed isomer, electron-donating substituents were expected to stabilize the excited state closed isomer, thereby explaining the red shifts in the absorbance and fluorescence spectra. Were these to be due only to induction and resonance of electron density favored by the substituent, the ideal relationship between σ' and absorbance maxima should be linear. Indeed, a linear correlation was observed between σ' and the absorbance or emission maxima (details of the fits can be found in the ESI†). However, no correlations could be established with either the absorption coefficients (in contrast to non-fluorescent diheteroarylethenes[34]) or with the fluorescence quantum yields.

The spectroscopic behaviour of compounds **3–8** was interpreted in the context of the PES model introduced above, incorporating some approximations based on the electron-donating character of the substituents. Donation of electron density to the central core of the diheteroarylethenes is assumed to have a stronger effect on the closed isomer than on the open isomer energy levels because of the absence of rotation of the benzothiophenes in the closed form and the

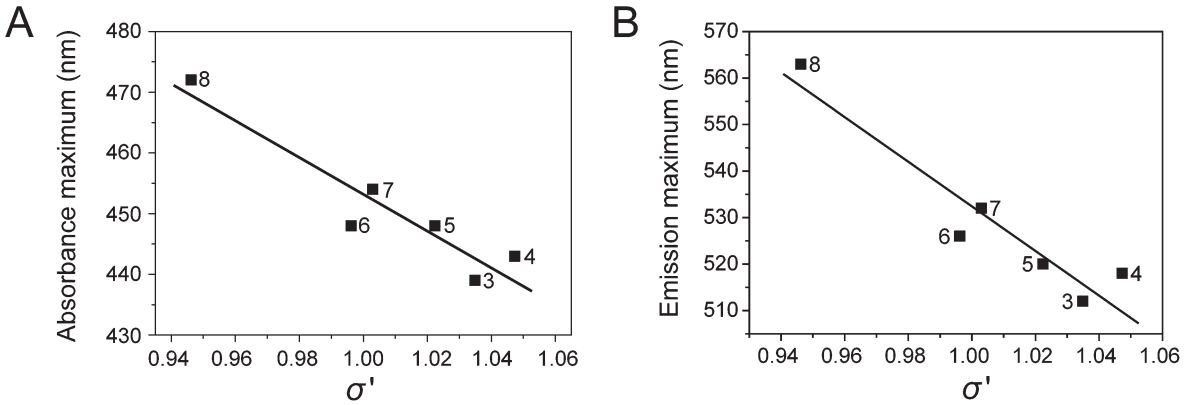

Fig. 2 Hammett correlations of σ' with (A) absorption maxima of the closed form and (B) fluorescence maxima of the closed form in 1,4-dioxane.

extension of the π network across the central core. In addition, electron-donation to the central core is thought to stabilize the excited state closed isomer relative to the ground state closed isomer, given the electronic rearrangement involved. We interpret the shift of absorption and fluorescence emission to longer wavelengths with increased electron-donating character as an immediate consequence of this phenomenon. As electron-donating substituents stabilize the π-electron conjugation in the closed isomer, compounds with stronger electron-donating substituents are expected to generate a more planar, less flexible aryl ring system. In conformity with this reasoning, an increase in fluorescence lifetime and a simultaneous albeit smaller decrease in calculated[35] non-radiative kinetic constants were observed with increasing electron-donating character (see the Photoconversion section).

The solvent dependence of the spectroscopic properties of **3–8** was studied by measuring the latter in a range of solvents. The results for the closed isomers **3c** (in the representation of compounds **4c–7c**) and **8c** are listed in Table 2. The data for all other compounds can be found in Table S1.† As can be seen in Fig. 3A, only weak solvatochromism was observed for **3–7**; there were only small shifts of 15 to 30 nm in the fluorescence maxima between heptane and methanol. The same phenomenon applied to the absorbance spectra. In fact, the absorbance maxima of the closed isomers were either unaffected or even shifted slightly to the blue upon passing from heptane to methanol, as is the case for compound **3c**. The peak absorbance wavelengths for the open isomers of compounds **3–7** did not shift considerably either; for **3o**, no shift was detected in going from heptane to methanol (Table S2†). These results are in accordance with prediction; neither a strong charge separation nor a substantial electronic dipole was expected to arise after excitation because of the similarity of the ground and excited state closed isomer geometries. Surprisingly, however, compound **8** showed a pronounced solvatochromic response (Fig. 3A and B). The emission band for this compound widened with greater solvent polarity and the Stokes shifts increased from 71 nm (2967 cm^{-1}) in heptane to 127 nm (4247 cm^{-1}) in acetonitrile. The shift in the fluorescence maximum was also a substantial 88 nm between heptane and acetonitrile. The change in fluorescence emission of **8c** from green in heptane to reddish-orange in methanol was observable by the naked eye (Fig. 3).

A typical solvatochromic dye with an absorbance maximum similar to that of **8c** is diethylamino-7-nitrobenz-2-oxa-1,3-diazol-4-yl[51] (diethylamino-NBD), as is indicated in a comparison of commonly used solvatochromic dyes compiled by Giordano *et al.*[49] Diethylamino-NBD has a Stokes shift value of 60 nm (2288 cm^{-1}) in acetonitrile and its solvatochromism from 1,4-dioxane to acetonitrile is 12 nm (416 cm^{-1}). The

Table 2 Solvent dependence of spectroscopic properties of **3c** and **8c**

		3c				**8c**			
Solvent	E_T^N	λ_{max} (nm), ε (mM^{-1} cm^{-1})	λ_{max}^{em} (nm)	Φ_f	τ_f (ns)	λ_{max} (nm), ε (mM^{-1} cm^{-1})	λ_{max}^{em} (nm)	Φ_f	τ_f (ns)
Heptane	0.012	437, 18	501	0.04	2.5	455, 32	526	0.65	2.3
Dioxane	0.164	431, 34	512	0.50	2.1	472, 44	563	0.56	2.4
THF	0.207	437, 35	514	0.52	—	479, 38	585	0.57	2.2
AcOEt	0.228	436, 36	511	0.29	1.1	472, 40	589	0.57	2.2
DCM	0.309	435, 38	508	0.45	—	472, 39	573	0.64	2.3
ACN	0.460	433, 35	515	0.17	—	487, 36	614	0.27	2.5
Methanol	0.762	428, 39	515	0.12	0.7	473, 36	603	0.42	2.2

E_T^N = normalized molar electronic transition energy;[47] λ_{max} = absorption maximum; ε = molar absorption coefficient; λ_{max}^{em} = fluorescence emission maximum; Φ_f = fluorescence quantum yield; τ_f = fluorescence lifetime.

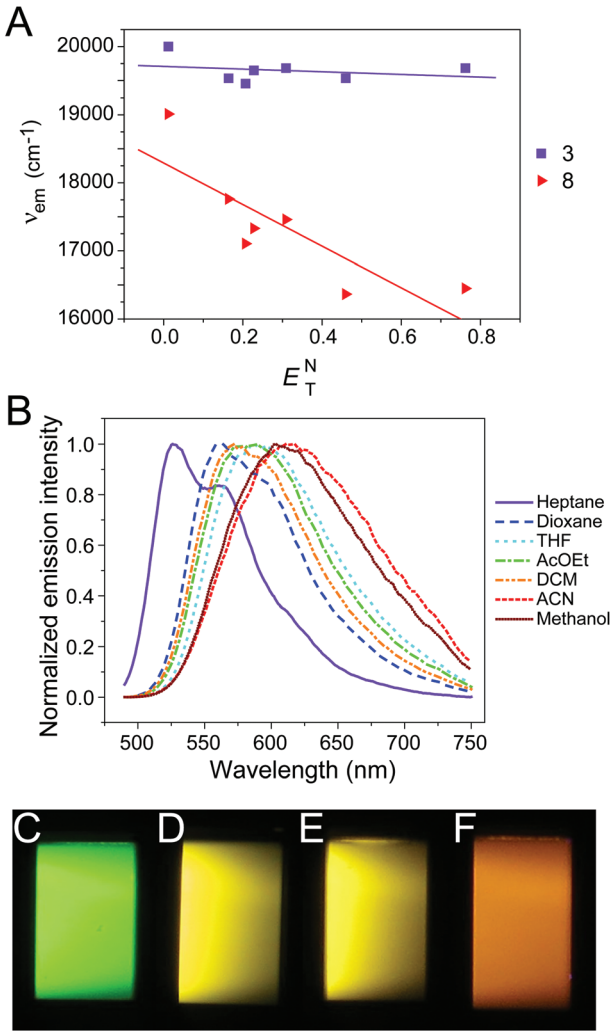

Fig. 3 (A) Maximum fluorescence emission frequency *vs.* solvent polarity scale (E_T^N) for compounds **3c** (representative of **4c–7c**) and **8c**. (B) Normalized emission spectra for **8c** in all solvents. Fluorescence emission of **8c** in (C) heptane, (D) 1,4-dioxane, (E) ethyl acetate and (F) methanol excited at 445 nm.

values for **8c** in the same solvents were 127 nm (4247 cm^{-1}), Stokes shift, and 51 nm (1476 cm^{-1}), solvatochromism. The solvatochromic response of **8c** was more than double that of diethylamino-NBD, accompanied by a much larger Stokes shift, classifying it as a superior solvatochromic probe for the given absorption range, unique as well in view of its photoactivatable nature.

For all compounds and in all solvents, the shifts in the absorbance maxima were smaller than those in fluorescence, indicating that the excited state closed isomer is more polar than the closed isomer in the ground state, and is therefore more stabilized by polar solvents. Furthermore, a slightly larger Stokes shift was observed in more polar solvents, indicating the existence of a stronger dipole moment in the excited state and therefore stronger interaction with polar solvents. Lippert–Mataga graphs[52] plotting the Stokes shifts against the solvent orientation polarizability (section 6 of the ESI†) clearly show this phenomenon. The regressions were roughly linear and specific-interaction dependent deviations were not observed. However a greater sensitivity of the compound to solvent polarity was found with increased electron-donating character (Fig. S2†). It has been suggested that non-oxidized diheteroarylethenes with reasonably comparable structures to compounds **3–8** present charge separation between the perfluorocyclopentene structure (acceptor) and the substituent group (donor),[53] accounting for their response to varying solvent polarity. A similar polarization of the molecules can be assumed for **3c–8c**, whereby electronic density is displaced towards the central core and perfluorocyclopentene structure from the substituents on the aryl rings. Such a polarization of the electronic cloud would create a larger dipole moment and be stabilized by polar solvents, thereby explaining the larger observed Stokes shift.

Catalán regressions carried out with absorbance maxima data did not comply with the goodness of fit requisite and thus the absorbance wavelengths for these compounds were not considered to depend on the nature of the solvent. Although solvent acidity and basicity parameters c_{SA} and d_{SB} appeared to have specific effects on some compounds (Table S6,† **4c** is slightly responsive to solvent acidity whereas **5c** and **8c** are slightly responsive to solvent basicity) no general tendency could be identified. Surprisingly, a relationship between solvent polarizability and (any of) the photophysical properties was also absent. However, the fluorescence emission maximum was seen to correlate rather strongly with solvent dipolarity, in accordance with the Lippert–Mataga analyses; values of b_{SdP} for each compound are plotted against the Hammett constant σ' in Fig. 4B. For a fluorophore with a polar excited state, solvents with large dipoles will significantly promote relaxation, inducing a larger shift in the fluorescence maximum. In particular, **8c** has the largest (absolute) value of b_{SdP}, supporting the assumption that the excited state for this compound is very polarized due to the electron-donating character of the ethoxybromo group.

The fluorescence lifetimes also presented some dependence on solvent polarity (Fig. 4A). Interestingly, the decrease in fluorescence lifetimes with solvent polarity was enhanced by more electron-withdrawing substituents; for example, for compound **3c**, τ_f was 2.5 ns in heptane and 0.7 ns in methanol. However, the lifetime of the most electron-donating substituted compound **8c** was much less sensitive to changes in the polarity of the environment. Fluorescence lifetimes were also examined with the Catalán regression (Fig. 4C, Table S6†) to identify parameters responsible for this variation. As in the case of the emission maxima, an interesting relationship between lifetimes and solvent dipolarity was observed. Whereas the lifetimes of compounds **3c–7c** were heavily dependent on the solvent polarity, that of compound **8c** was not; an explanation for these results is offered in the next section.

Photoconversion

The reversible photoconversion of diheteroarylethenes between two thermally stable isomers is one of their great

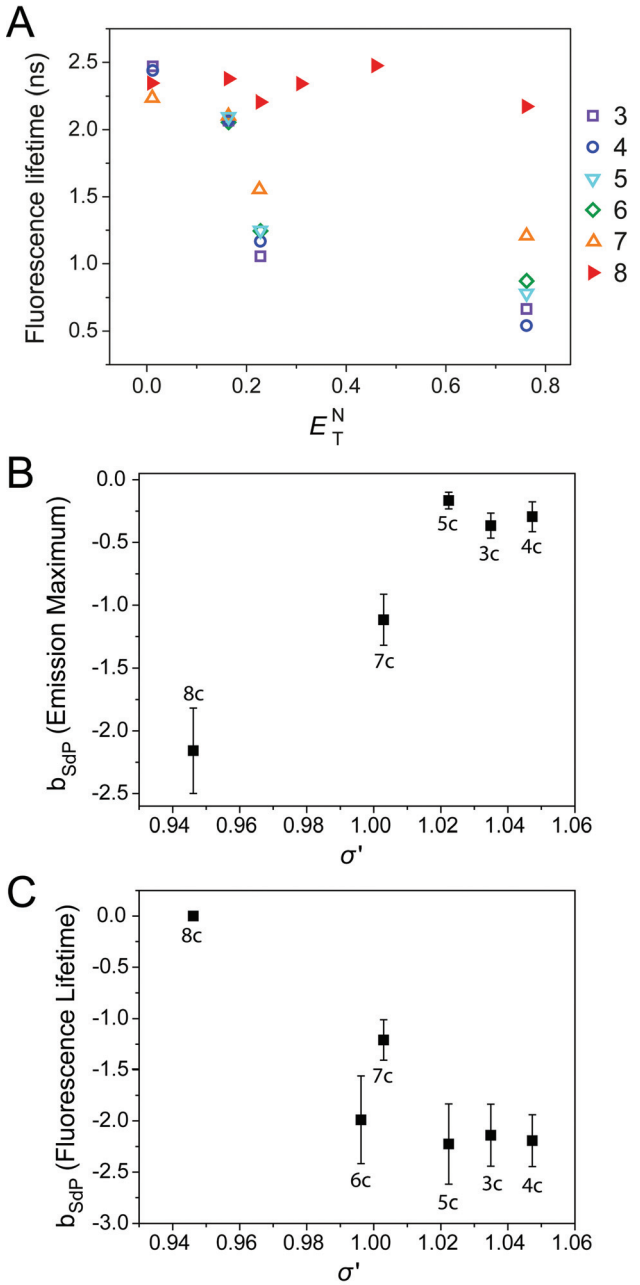

Fig. 4 (A) Fluorescence lifetime *vs.* solvent polarity scale E_T^N for compounds **3c–8c**. (B) Catalán solvent dipolarity parameter b_{SdP} for fluorescence emission maxima *vs.* Hammett constant σ'. The linear regression of compound **6c** had $R^2 < 0.8$ and was excluded. (C) Catalán solvent dipolarity parameter b_{SdP} for fluorescence lifetimes *vs.* Hammett constant σ'. The linear regression of compound **8c** is independent of solvent polarity. Error bars in (B) and (C) show the standard error of the fit.

advantages over thermally reverting photochromes. Table 3 shows the cyclization and cycloreversion parameters for compounds **3–8**. The quantum yields of cycloreversion ($\Phi_{c\rightarrow o}$), induced by exposure to visible light, were at least two orders of magnitude lower than the cyclization quantum yields ($\Phi_{o\rightarrow c}$), as has been shown for other diheteroarylethenes.[29,35] In addition,

Table 3 Photoconversion properties for **3–8** in ethyl acetate

	$\Phi_{o\rightarrow c}$	$10^3\ \Phi_{c\rightarrow o}$	k_f (ns^{-1})	k_{nr} (ns^{-1})	$k_{c\rightarrow o}$ (μs^{-1})
3	0.50	4.9	0.27	0.67	4.6
4	0.37	1.9	0.29	0.56	1.6
5	0.45	1.1	0.16	0.64	0.85
6	0.27	0.46	0.25	0.55	0.37
7	0.44	0.35	0.20	0.44	0.22
8	0.010	a	0.26	a	a

$\Phi_{c\rightarrow o}$, cycloreversion quantum yield under irradiation at 445 nm; k_f = radiative decay rate constant; k_{nr} = non-radiative decay rate constant; $k_{c\rightarrow o}$ = cycloreversion rate constant; a = too low to measure. Calculated according to ref. 35; see section 8 of ESI for a detailed explanation.

$\Phi_{o\rightarrow c}$ decreased as the electron-donating character increased. In particular, for compound **8**, photoreversion was so inefficient that a quantum yield could not be determined for this reaction by absorption spectrometry. In practical terms, **3–7** are reversibly photoswitchable, whereas **8** only undergoes photocyclization. The compounds were subjected to many cycles of photocyclization–photoreversion with little photodegradation (Fig. S4†). Compound **5** withstood more than 25 hours of UV irradiation at ~10 mW cm^{-2} in ethyl acetate while maintaining more than 50% fluorescence (Fig. S5†). This fatigue resistance is greater than twice that of compound **1**.[54]

Guillaumont *et al.*[42] have proposed a relationship between experimental $\Phi_{o\rightarrow c}$ and $\Phi_{c\rightarrow o}$ and substituent effects in the case of non-oxidized diheteroarylethenes. Stabilization of the excited state closed isomer increases the transition energy required to pass over into the excited state open isomer minimum and therefore hinders the photoreversion back to the open form. $\Phi_{c\rightarrow o}$ decreased from 4.9×10^{-3} for **3** to 3.5×10^{-4} for **7** (compound **8** had a much smaller $\Phi_{c\rightarrow o}$ that could not be determined) and the cycloreversion kinetic constants decreased over 10-fold from **3** to **7**. Hammett correlations show that the $\Phi_{c\rightarrow o}$ decreased with electron-donating character, in agreement with the data for non-fluorescent diheteroarylethenes.[34] The stabilization of the closed isomer does not directly affect the cyclization pathway; accordingly, $\Phi_{o\rightarrow c}$ did not vary systematically with the electron-donating character of compounds **3–7**. However, there was a drastic decrease in $\Phi_{o\rightarrow c}$ for compound **8**, which is somewhat more difficult to rationalize. A possible explanation for this phenomenon would be that the electron-donating substituent modifies the potential energy surface (particularly that of the excited state) such that the position of the CI involved is slightly altered (Scheme 3), favoring decay to the open isomer from the excited state open isomer and therefore leading to a lower cyclization quantum yield. Another possibility is an increase in the non-radiative decay after excitation of the open isomer. Further theoretical studies are needed to estimate the nature of the changes in the potential energy surfaces.

Although the solvent identity did not affect the spectroscopic properties of compounds **3–7**, this was not the case for

the photoconversion. **8c** had a negligible $\Phi_{c\to o}$ such that a large activation energy for the transition from the closed to the open excited states must be assumed. If the transition energy is very large even in non-polar solvents, solvent polarity will not have a substantial effect on the favored decay pathways from the excited state back to the ground state. This situation is reflected in the stability of the fluorescence lifetimes of **8c** across the range of solvents. In contrast, compounds **3c–7c** presented much shorter fluorescence lifetimes in polar solvents, yet the $\Phi_{c\to o}$ were unaltered (Table 4). Decay rate constant calculations (Table S3†) indicate that the shorter lifetime of compound **3c** in more polar solvents reflects the increases in both the cycloreversion and non-radiative decay constants. As these pathways are more accessible (the activation energy for cycloreversion is smaller), relatively small changes in the energy levels of the closed and open excited states and the transition state affect the favored decay pathways to a greater degree, explaining the substantial influence of solvent dipolarity on fluorescence lifetime.

No correlation of $\Phi_{o\to c}$ with solvent polarity was found for **3** (representative of **4–7**); however, for **8**, $\Phi_{o\to c}$ decreased almost 1000-fold in polar solvents (0.31 in heptane to 0.0004 in acetonitrile). One explanation would be that polar solvents affect the equilibrium between the parallel and anti-parallel conformers, which in turn affects the cyclization kinetics. The parallel conformer was found to be slightly favored in methanol as compared to chloroform, increasing from 47% to 54% (determined by ^{1}H NMR), but this minor effect cannot account for the dramatic decrease in $\Phi_{o\to c}$. The Catalán regression performed with the $\Phi_{o\to c}$ of **8c** is given in eqn (2).

$$\Phi^{8}_{o\to c} = (0.33 \pm 0.02) - (0.25 \pm 0.02)\mathrm{SdP} + (0.10 \pm 0.03)\mathrm{SA} - (0.30 \pm 0.03)\mathrm{SB} \quad (2)$$

An increase in both solvent dipolarity and solvent basicity was correlated with decreased quantum yield, whereas greater solvent acidity correlated with increased $\Phi_{o\to c}$, albeit to a lesser degree. These effects are clearly seen in the increase of $\Phi_{o\to c}$ in dichloromethane, a solvent that is slightly more acidic and considerably less basic than ethyl acetate. It is probable that the sulfone groups on the benzothiophene rings contribute to these specific solvent effects and further investigation with a wider range of solvents is necessary to elucidate the basis for the changes in solvent acidity or basicity on the cyclization mechanism. $\Phi_{o\to c}$ of **8** depends greatly on the solvent dipolarity, once again pointing to a highly polarized molecule whose energy levels are influenced greatly by the polarity of the environment.

Table 4 Cyclization and cycloreversion quantum yields for compounds **3** and **8** in different solvents

	3		**8**
Solvent	$\Phi_{o\to c}$	$10^3\ \Phi_{c\to o}$	$10^3\ \Phi_{o\to c}$
Heptane	0.37	6.2	310
Dioxane	0.51	2.6	100
THF	0.44	3.1	9.4
AcOEt	0.50	4.9	9.6
DCM	0.32	3.4	84
ACN	0.52	4.5	0.4
Methanol	0.34	3.1	1.2

$\Phi_{o\to c}$, cyclization quantum yield under irradiation at 340 nm; $\Phi_{c\to o}$, cycloreversion quantum yield under irradiation at 445 nm. $\Phi_{c\to o}$ for compound **8** was too low to measure by absorption spectroscopy. See section 8 of ESI for a detailed explanation of the calculations.

Conclusions

We have studied the effect of substituents on the photophysical properties of fluorescent diheteroarylethenes by incorporating electron-donating functional groups in position *para* to positions 6 and 6′ of the benzothiophenes. As the electron-donating character increased, absorbance and emission bands shifted towards longer wavelengths, but no significant effect on the fluorescence quantum yields was observed. However, the photoconversion properties were substantially affected by electron-donating substituents. The cyclization and cycloreversion quantum yields decreased to such an extent that it was practically impossible to induce photoreversion in the case of strong electron-donating substituents, which are proposed to stabilize the excited state closed isomer. Despite the weak solvatochromism of the majority of the compounds studied, a reduction in fluorescence lifetime with increasing solvent polarity was observed for all compounds, supposedly due to an increase in both cycloreversion and non-radiative decay. Compound **8**, with an electron-donating ethoxybromo substituent, also displayed a marked solvatochromism, with a shift of 86 nm in passing from heptane to acetonitrile. Compound **8** is thus one of the very few reported[14] solvatochromic photoactivatable fluorescent small organic probes. The combination of low fatigue, rapid photoswitching, the possibility for cycling the dyes numerous times between the on and off states and their relatively large fluorescence quantum yields (up to 0.57) renders the probes described in this communication good candidates for use in super-resolution microscopy. Reactivity for biomolecules and derivatization to confer improved solubility and photoconvertibility in water are the goals of current investigation.

Experimental section

General procedures

All reagents and solvents were acquired from commercial suppliers and used without further purification. The boronic acids were obtained from Combi-Blocks Inc. Column chromatography was performed with silica gel (Merck Silica 60, particle size 0.040–0.063 mm or Merck Silica 60, 230–400 mesh). Solvents for spectral measurements were of spectroscopic grade.

^{1}H and ^{13}C NMR spectra were recorded in $CDCl_3$ on an Agilent 400-MR spectrometer and on a Varian Inova 500 MHz spectrometer. Residual undeuterated solvent was used as an internal standard (7.26 ppm for ^{1}H, 77.16 ppm for ^{13}C). High resolution mass spectrometry was carried out on a microTOF focus instrument, Bruker Daltronik GmbH (ESI-HRMS).

Spectroscopic measurements

Samples were irradiated using a Hg arc lamp (SUV-DC, Lumatec, Deisenhofen, Germany) and band pass filters (340 ± 10 nm, 445 ± 20 nm). For all spectroscopic measurements, closed quartz Hellma 3 × 3 mm microcuvettes were used and filled such that the entire sample was exposed to light, eliminating mixing effects. Stirring of the sample was performed during constant UV irradiation in photodegradation experiments and during cyclization and cycloreversion quantum yield determinations. Internal filter effects were avoided by use of concentrations ≤10 μM). The proportion of open and closed isomers was unaffected by the light levels used for monitoring the system. Absorbance spectra (250–800 nm) were acquired on a Cary 100 UV-vis spectrophotometer (Varian) utilizing microcuvettes with a 3 mm optical path. Fluorescence spectra were acquired on a Cary Eclipse fluorescence spectrophotometer (Varian) utilizing the same microcuvettes. Excitation and emission bandwidths were 5 nm, and the sample temperature was 20 °C. For cyclization and cycloreversion quantum yield determinations, a lab designed absorption/fluorescence spectrometer with built-in photoconversion capabilities was used (for a more detailed description see ESI†). Fluorescence lifetime measurements were performed on a FluoroLog-TCSPC (Horiba Jobin Yvon). Excitation was carried out using a nanoLED N-460 nm source (Horiba Scientific), a temporal window of 50 ns, a pulse repetition frequency of 1 MHz, and ≥2000 peak counts. Emission counts were determined at the respective fluorescence maxima. Mean lifetimes were calculated using one component fitting (closed isomers) with *Mathematica* software. Catalan parameters were also calculated using *Mathematica* software (further details in ESI†).

Synthesis

Compounds **1** and **2** were obtained according to published procedures.[27] Compounds **3–8** were prepared according to Scheme 1; synthetic procedures can be found in the ESI.†

Conflict of interest

The authors declare no competing financial interests.

Acknowledgements

This manuscript is dedicated to the memory of Elizabeth Jares-Erijman, first research supervisor of PhD student F.G. We thank the Department of Physical Biochemistry, MPIbpc, for the use of the TCSPC fluorimeter; the Facility for Synthetic Chemistry, MPIbpc, for HPLC separations and NMR spectra; and the Analytic and Mass-Spectrometry Center and NMR-Service, Georg-August University in Göttingen, for mass and NMR spectra. We also thank Anthony de Vries and Stephen Gillanders for their assistance in the construction of the custom spectrometer. This work was supported by the Max Planck Society and the German BMBF (CIRM FKZ 1316050). F.G. received a joint fellowship from the Ministerio de Educación de la República Argentina and the Deutscher Akademischer Austauschdienst (#A/11/75379).

Notes and references

1 S. W. Hell, *Science*, 2007, **316**, 1153–1158.
2 B. Huang, *Curr. Opin. Chem. Biol.*, 2010, **14**, 10–14.
3 T. Müller, C. Schumann and A. Kraegeloh, *ChemPhysChem*, 2012, **13**, 1986–2000.
4 L. Shao, P. Kner, E. H. Rego and M. G. L. Gustafsson, *Nat. Methods*, 2011, **12**, 1044–1046.
5 A. G. York, S. H. Parekh, D. Dalle Nogare, R. S. Fischer, K. Temprine, M. Mione, A. B. Chitnis, C. A. Combs and H. Shroff, *Nat. Methods*, 2012, **9**, 749–754.
6 D. S. Lidke and K. A. Lidke, *J. Cell Sci.*, 2012, **125**, 2571–2580.
7 T. Dertinger, R. Colyer, G. Iyer, S. Weiss and J. Enderlein, *Proc. Natl. Acad. Sci. U. S. A.*, 2009, **106**, 22287–22292.
8 C. B. Müller and J. Enderlein, *Phys. Rev. Lett.*, 2010, **104**, 198101.
9 J. Vogelsang, T. Cordes, C. Forthmann, C. Steinhauer and P. Tinnefeld, *Nano Lett.*, 2010, **10**, 672–679.
10 D. M. Owen, D. J. Williamson, A. Magenau and K. Gaus, *Nat. Commun.*, 2012, **3**, 1256.
11 M. Lakadamyali, H. Babcock, M. Bates, X. Zhuang and J. Lichtman, *PloS One*, 2012, **7**, e30826.
12 R. Henriques, C. Griffiths, E. Hesper Rego and M. M. Mhlanga, *Biopolymers*, 2011, **95**, 322–331.
13 T. Ha and P. Tinnefeld, *Annu. Rev. Phys. Chem.*, 2012, **63**, 595–617.
14 S. J. Lord, N. R. Conley, H.-L. D. Lee, S. Y. Nishimura, A. K. Pomerantz, K. A. Willets, Z. Lu, H. Wang, N. Liu, R. Samuel, R. Weber, A. Semyonov, M. He, R. J. Twieg and W. E. Moerner, *ChemPhysChem*, 2009, **10**, 55–65.
15 D. Bourgeois, A. Regis-Faro and V. Adam, *Biochem. Soc. Trans.*, 2012, **40**, 531–538.
16 K. Finan, B. Flottmann and M. Heilemann, in *Methods in molecular biology*, ed. A. A. Sousa and M. J. Kruhlak, Humana Press, Totowa, NJ, 2013, vol. 950, pp. 131–151.
17 C.-J. Carling, J.-C. Boyer and N. R. Branda, *Org. Biomol. Chem.*, 2012, **10**, 6159–6168.
18 F. May, M. Peter, A. Hütten, L. Prodi and J. Mattay, *Chem.–Eur. J.*, 2012, **18**, 814–821.
19 T. Klein, S. van de Linde and M. Sauer, *ChemBioChem*, 2012, **13**, 1861–1863.

20 K. Kolmakov, C. Wurm, M. V. Sednev, M. L. Bossi, V. N. Belov and S. W. Hell, *Photochem. Photobiol. Sci.*, 2012, **11**, 522–532.
21 P. Schäfer, S. van de Linde, J. Lehmann, M. Sauer and S. Doose, *Anal. Chem.*, 2013, **85**, 3393–3400.
22 M. Schwering, A. Kiel, A. Kurz, K. Lymperopoulos, A. Sprödefeld, R. Krämer and D.-P. Herten, *Angew. Chem., Int. Ed.*, 2011, **50**, 2940–2945.
23 G. M. Hagen, W. Caarls, K. A. Lidke, A. H. B. De Vries, C. Fritsch, B. G. Barisas, D. J. Arndt-Jovin and T. M. Jovin, *Micros. Res. Tech.*, 2009, **72**, 431–440.
24 L. Giordano, T. M. Jovin, M. Irie and E. A. Jares-Erijman, *J. Am. Chem. Soc.*, 2002, **124**, 7481–7489.
25 S. A. Díaz, L. Giordano, T. M. Jovin and E. A. Jares-Erijman, *Nano Lett.*, 2012, **12**, 3537–3544.
26 Y. Yan, M. E. Marriott, C. Petchprayoon and G. Marriott, *Biochem. J.*, 2011, **433**, 411–422.
27 K. Uno, H. Niikura, M. Morimoto, Y. Ishibashi, H. Miyasaka and M. Irie, *J. Am. Chem. Soc.*, 2011, **133**, 13558–13564.
28 J. Qiu, L. Wang, M. Liu, Q. Shen and J. Tang, *Tetrahedron Lett.*, 2011, **52**, 6489–6491.
29 Y.-C. Jeong, S. I. Yang, K.-H. Ahn and E. Kim, *Chem. Commun.*, 2005, **19**, 2503–2505.
30 G. Liu, S. Pu and X. Wang, *Tetrahedron*, 2010, **66**, 8862–8871.
31 S. Pu, R. Wang, G. Liu, W. Liu, S. Cui and P. Yan, *Dyes Pigm.*, 2012, **94**, 195–206.
32 K. Morimitsu and S. Kobatake, *Mol. Cryst. Liq. Cryst.*, 2005, **431**, 151–154.
33 S. Pu, C. Fan, W. Miao and G. Liu, *Dyes Pigm.*, 2010, **84**, 25–35.
34 M. Irie, K. Sakemura, M. Okinaka and K. Uchida, *J. Org. Chem.*, 1995, **60**, 8305–8309.
35 Y. Takagi, T. Kunishi, T. Katayama, Y. Ishibashi, H. Miyasaka, M. Morimoto and M. Irie, *Photochem. Photobiol. Sci.*, 2012, **11**, 1661–1665.
36 C. Hansch, A. Leo and W. Taft, *Chem. Rev.*, 1991, **91**, 165–195.
37 L. P. Hammett, *Struct. React. Benzene Compounds*, 1937, **59**, 96–103.
38 H. Neuvonen, K. Neuvonen, A. Koch, E. Kleinpeter and P. Pasanen, *J. Org. Chem.*, 2002, **67**, 6995–7003.
39 R. Contreras, J. Andrés, L. R. Domingo, R. Castillo and P. Pérez, *Tetrahedron*, 2005, **61**, 417–422.
40 Spectral Database for Organic Compounds (National Institute of Advanced Industrial Science and Technology) http://riodb01.ibase.aist.go.jp/sbds/ (accessed November 29, 2012).
41 X. Cui, Y. Zhang, F. Shi and Y. Deng, *Chemistry*, 2011, **17**, 1021–1028.
42 D. Guillaumont, T. Kobayashi, K. Kanda, H. Miyasaka, K. Uchida, S. Kobatake, K. Shibata, S. Nakamura and M. Irie, *J. Phys. Chem. A*, 2002, **106**, 7222–7227.
43 Y. Asano, A. Murakami, T. Kobayashi, A. Goldberg, D. Guillaumont, S. Yabushita, M. Irie and S. Nakamura, *J. Am. Chem. Soc.*, 2004, **126**, 12112–12120.
44 M. Boggio-Pasqua, M. Ravaglia, M. J. Bearpark, M. Garavelli and M. A. Robb, *J. Phys. Chem. A*, 2003, **107**, 11139–11152.
45 Y. Ishibashi, T. Umesato, S. Kobatake, M. Irie and H. Miyasaka, *J. Phys. Chem. C*, 2012, **116**, 4862–4869.
46 S. M. Polyakova, V. N. Belov, M. L. Bossi and S. W. Hell, *Eur. J. Org. Chem.*, 2011, 3301–3312.
47 C. Reichardt, *Chem. Rev.*, 1994, **94**, 2319–2358.
48 J. Catalán, *J. Phys. Chem. B*, 2009, **113**, 5951–5960.
49 L. Giordano, V. V. Shvadchak, J. A. Fauerbach, E. A. Jares-Erijman and T. M. Jovin, *J. Phys. Chem. Lett.*, 2012, **3**, 1011–1016.
50 Y.-C. Jeong, D. G. Park, I. S. Lee, S. I. Yang and K.-H. Ahn, *J. Mater. Chem.*, 2009, **19**, 97–103.
51 S. Fery-Forgues, J.-P. Fayet and A. Lopez, *J. Photochem. Photobiol., A: Chem.*, 1993, **70**, 229–243.
52 J. R. Lakowicz, *Principles of Fluorescence Spectroscopy*, Kluwer Academic/Plenum Publishers, New York, U.S.A., 2nd edn, 1999.
53 S. Kobatake, Y. Terakawa and H. Imagawa, *Tetrahedron*, 2009, **65**, 6104–6108.
54 Y.-C. Jeong, S. I. Yang, E. Kim and K.-H. Ahn, *Tetrahedron*, 2006, **62**, 5855–5861.

